ANNALS of Clinical and Translational Neurology
Open Access
ANA American Neurological Association since 1875

RESEARCH ARTICLE

Alternative splicing in a presenilin 2 variant associated with Alzheimer disease

Jacquelyn E. Braggin[1], Stephanie A. Bucks[1], Meredith M. Course[2], Carole L. Smith[1], Bryce Sopher[1], Leah Osnis[1], Kiel D. Shuey[1], Kimiko Domoto-Reilly[1], Christina Caso[1], Chizuru Kinoshita[3], Kathryn P. Scherpelz[4], Chloe Cross[5], Thomas Grabowski[1,6], Seyyed H. M. Nik[7], Morgan Newman[7], Gwenn A. Garden[1,4], James B. Leverenz[8], Debby Tsuang[1,2,9,10], Caitlin Latimer[4], Luis F. Gonzalez-Cuyar[4], Christopher Dirk Keene[4], Richard S. Morrison[3], Kristoffer Rhoads[1], Ellen M. Wijsman[2,11], Michael O. Dorschner[4,9,12], Michael Lardelli[7], Jessica E. Young[4], Paul N. Valdmanis[2], Thomas D. Bird[1,2,10] & Suman Jayadev[1,2]

[Correction added on 25 March 2019 after first online publication on 10 March 2019: The author's name Christopher Dirk Keene has been corrected.]

[1]Department of Neurology, University of Washington, Seattle, Washington
[2]Division of Medical Genetics, Department of Medicine, University of Washington, Seattle, Washington
[3]Department of Neurological Surgery, University of Washington, Seattle, Washington
[4]Department of Pathology, University of Washington, Seattle, Washington
[5]School of Medicine, University of Utah, Salt Lake City, Utah
[6]Department of Radiology, University of Washington, Seattle, Washington
[7]Genetics and Evolution, University of Adelaide, Adelaide, South Australia
[8]Cleveland Lou Ruvo Center for Brain Health, Cleveland, OH
[9]Department of Psychiatry & Behavioral Sciences, University of Washington, Seattle, Washington
[10]Geriatric Research, Education, and Clinical Center, VA Puget Sound Health Care System, Seattle, Washington
[11]Univeristy of Washington Department of Biostatistics, Seattle, Washington
[12]UW Medicine Center for Precision Diagnostics, University of Washington, Seattle, Washington

Correspondence
Suman Jayadev, Department of Neurology, Arthur Krause Professorship for Neurogenetics Research, Clinical Core Leader, UW Alzheimer Disease Research Center, University of Washington Medical Center, Seattle, WA 98195. Tel: (206) 221-2930; Fax: 206-685-8100; E-mail: sumie@uw.edu

Funding Information
This work was supported by the Bright Focus Foundation (grant/award number: 'A88973'), National Institutes of Health (grant/award number: 'AG062903'), National Institute on Aging (grant/award number: '1R01AG053002', 'K02 AG04447', 'P50 AG05136'), Ellison Foundation, National Institute of General Medical Sciences (grant/award number: '5T32GM007454-42'), Australia's National Health and Medical Research Council (grant/award number: 'GNT1126422').

Received: 16 October 2018; Revised: 25 January 2019; Accepted: 12 February 2019

Abstract

Objective: Autosomal-dominant familial Alzheimer disease (AD) is caused by by variants in presenilin 1 (*PSEN1*), presenilin 2 (*PSEN2*), and amyloid precursor protein (*APP*). Previously, we reported a rare *PSEN2* frameshift variant in an early-onset AD case (PSEN2 p.K115Efs*11). In this study, we characterize a second family with the same variant and analyze cellular transcripts from both patient fibroblasts and brain lysates. **Methods**: We combined genomic, neuropathological, clinical, and molecular techniques to characterize the PSEN2 K115Efs*11 variant in two families. **Results**: Neuropathological and clinical evaluation confirmed the AD diagnosis in two individuals carrying the PSEN2 K115Efs*11 variant. A truncated transcript from the variant allele is detectable in patient fibroblasts while levels of wild-type *PSEN2* transcript and protein are reduced compared to controls. Functional studies to assess biological consequences of the variant demonstrated that PSEN2 K115Efs*11 fibroblasts secrete less Aβ_{1-40} compared to controls, indicating abnormal γ-secretase activity. Analysis of *PSEN2* transcript levels in brain tissue revealed alternatively spliced *PSEN2* products in patient brain as well as in sporadic AD and age-matched control brain. **Interpretation**: These data suggest that PSEN2 K115Efs*11 is a likely pathogenic variant associated with AD. We uncovered novel *PSEN2* alternative transcripts in addition to previously reported *PSEN2* splice isoforms associated with sporadic AD. In the context of a frameshift, these alternative transcripts return to the canonical reading frame with potential to generate

***Annals of Clinical and Translational Neurology* 2019; 6(4): 762–777**

doi: 10.1002/acn3.755

deleterious protein products. Our findings suggest novel potential mechanisms by which *PSEN* variants may influence AD pathogenesis, highlighting the complexity underlying genetic contribution to disease risk.

Introduction

Autosomal-dominant familial Alzheimer disease (FAD) is caused by heterozygous variants in presenilin 1 (*PSEN1*), presenilin 2 (*PSEN2*), or amyloid precursor protein (*APP*).[1] While earlier in onset, FAD is clinically and neuropathologically similar to the more common later onset "sporadic" form of AD. Thus, studying FAD contributes to understanding pathogenic mechanisms relevant to both Mendelian and complex sporadic AD.[2] To date, hundreds of *PSEN* variants have been reported and the vast majority are missense changes.[3] Presenilin protein (PS) forms the catalytic component of the transmembrane γ-secretase complex to process over 100 substrates including APP.[4] FAD-associated *PSEN* variants are hypothesized to alter the γ-secretase processing of APP, producing species of amyloid beta (Aβ) of varying solubility and aggregation potential that can be identified in amyloid plaques, a defining neuropathological feature of AD.[5] How *PSEN* variants lead to FAD is uncertain; controversy remains regarding the relative importance of a gain-of-function impact of *PSEN* variant by alteration of the quality of Aβ species and A$\beta_{42:40}$ ratios versus deleterious loss-of-function consequences of variants.[6–8]

In 2010, we reported the first case of a *PSEN2* two base-pair deletion, PSEN2 c.342_343delGA, p.K115Efs*11, identified in an early-onset AD case, suggesting this novel *PSEN2* variant may be a pathogenic cause of FAD.[9] The patient was diagnosed with AD at age 56 years but there was limited family history information to determine segregation in an autosomal-dominant inheritance pattern. Despite the early-onset of disease and in silico analysis suggesting pathogenicity, PSEN2 K115Efs*11 (PSEN2 K115fs) remained a variant of unknown significance given the unique presentation in one case.

Using targeted exome screening, we analyzed 135 archived samples from a cohort of early-onset familial AD cases at the University of Washington for known dementia genes, including *PSEN1*, *PSEN2*, and *APP*. During this study, we identified a second early-onset AD individual who also carried the PSEN2 K115fs variant.

We present here clinical and neuropathological data from two early-onset AD individuals carrying the PSEN2 K115fs variant whose families are not known to be related and are from distinct regions in the United States. We describe the clinical and neuropathological features of members in both families. We identified a novel splice isoform in PSEN2 K115fs patient brain lysate that was not readily detected in patient fibroblasts. PSEN2 K115fs patient-derived alternative splice isoforms are predicted to remain in frame, potentially generating a protein with large structural differences that could alter PS2 function and drive AD pathologic processes. Collectively, these data further support pathogenicity of this unusual variant and suggest additional complexity for FAD pathogenicity.

Materials and Methods

Fibroblast culture

Skin punch biopsies (3 mm) were obtained from all subjects giving informed consent under protocols approved by the University of Washington (UW) Institutional Review Board. Age-matched control lines were obtained from the UW Alzheimer Disease Research Center (ADRC). The PSEN2 K115fs (Family B proband) skin sample was obtained under an ADRC-affiliated UW Institutional Review Board approved protocol. Fibroblast lines were prepared either through the ADRC or University of Washington Cytology laboratory. Cell lines were maintained in fibroblast culture media (Dulbecco's Modified Eagle Medium [DMEM] supplemented with 10% fetal calf serum, 1% L-glutamine, 0.1% penicillin/streptomycin), and fibroblast lines from passage numbers 5 to 15 were used for experiments.

Neuropathology

The study was approved by the UW IRB; neuropathology diagnostic protocols aligned with NIA-AA guidelines.[10–14] Sections (5 μm) were prepared from formalin-fixed, paraffin-embedded sections, and histochemically stained for hematoxylin and eosin with Luxol fast blue and Bielschowsky, and immunohistochemistry using a Leica Bond III Autostainer (Leica Bio-Systems, Richmond, IL, USA) for paired helical filament tau (PHF-tau) (mouse, AT8, 1:1000, Pierce, Rockfield, IL, USA), phospho-tau (mouse, Tau 2, 1:1000, Sigma-Aldrich, St. Louis, MO, USA), Aβ (6E10) (mouse, 1:5000, Covance, Burlington, NC, USA), phosphorylated TDP-43 (pTDP43) (rat, ser409/ser410, 1:1000, Millipore, Burlington, MA, USA), α-synuclein (LB509, mouse, 1:500, Invitrogen, Carlsbad, CA, USA), GFAP (rabbit, 1:2000, DAKO, Santa Clara, CA, USA), and IBA-1 (rabbit, 1:1700, Wako, Richmond, VA, USA) with appropriate secondary antibody staining.

Molecular genetics

Exome sequencing

Libraries were constructed according to an optimized protocol developed by the UW Medicine Center for Precision Diagnostics and Northwest Clinical Genomics Laboratory. Sample-specific fragment libraries were prepared using the KAPA Hyper Prep DNA library kit (KAPA Biosystems, Wilmington, MA, USA) and subsequently enriched with the xGen Exome Research Panel v1.0 (Integrated DNA Technologies, Coralvilla, IA, USA). The standard off-the-shelf probe set was supplemented with baits to capture missing targets, and boost coverage of poorly covered targets. Paired-end sequencing of the exome-enriched libraries was performed on a HiSeq 4000 instrument (Illumina, San Diego, CA, USA) according to the manufacturer's protocol.

Sanger sequencing

Primers based on the GRCh37/hg19 (February 2009) version of the human genome sequence were used to amplify a region containing the PSEN2 K115Efs*11 region (Table 2). Polymerase chain reaction (PCR)-amplified fragments were sequenced using standard dye-terminator chemistry and separated on an ABI 3500 Genetic Analyzer (Applied Biosystems, Foster City, CA, USA). Resulting traces were analyzed using Mutation Surveyor v5.0 (SoftGenetics, State College, PA, USA).

Three-dimensional quant studio dPCR

Digital PCR (dPCR) allows accurate quantification of nucleic acid templates by partitioning the PCR reaction mix over a large number of wells, so that each well contains a single copy or no copies of the target region.[15] Based on the assumption of Poisson distribution of copies, the number of template copies originally present in the sample can be recalculated from the number of wells in which amplification has successfully occurred. dPCR was performed on a QuantStudio™ 3D Digital PCR System (Life Technologies, Carlsbad, CA, USA). We prepared 20 μL reaction mixes containing 9 μL 1X QuantStudio™ 3D digital PCR Master Mix (Life Technologies), 2 μL of 20X Sybr® dye in TE buffer, 50 ng cDNA in total reaction, 200 nmol/L of specific primers, and 6.3 μL of nuclease-free water (Qiagen, Germantown, MD, USA). We loaded 14.5 μL of the reaction mixture onto a QuantStudio™ 3D digital PCR 20 K chip (Life Technologies) using an automatic chip loader (Life Technologies) according to manufacturer's instructions. The chip is divided into 20,000 consistently sized reaction wells in which the nucleic acid mixture was randomly divided. Loaded chips underwent thermocycling on the Gene Amp 9700 PCR system under following conditions: 96°C for 10 min, 45 cycles of 60°C for 2 min, and at 98°C for 30 sec, followed by a final extension step at 60°C for 2 min. After thermocycling, the chips were imaged on a QuantStudio™ 3D instrument, which assesses raw data and calculates the estimated concentration of the nucleic acid sequence targeted by the FAM™ dye labeled probes by Poisson distribution.[16]

RT-PCR

RNA was isolated using an RNeasy® Lipid Tissue Mini Kit (74804, Qiagen) from parietal cortex. *PSEN2* levels (total, exon 6 deletion [PS2V], and partial intronic retention [+77 bp]) were measured in a QuantStudio version 3 real-time PCR system (Thermo Fisher Scientific, Waltham, MA, USA) and normalized to a standard curve generated using cloned vectors DNA containing the wild-type, PS2V, and +77 bp-specific *PSEN2* cDNAs. Assay on Demand (Applied Biosystems) kits were employed to measure *Notch1* (Hs01062014_m1), *APP* (Hs00169098_m1), Hes1 (Hs00172878_m1), and ACTB (Hs99999903_m1) by real-time PCR. Fold changes were calculated using the ΔΔ-CT method against beta-actin housekeeping gene.

Western blot analysis

Human fibroblasts were passaged in fibroblast culture medium and lysed in cell lysis buffer (Cell Signaling Technology, Danvers, MA) containing protease inhibitors and separated by sodiumdodecyl sulfate (SDS)–polyacrylamide gel electrophoresis using β-mercaptoethanol (Bio-Rad Laboratories, Hercules, CA), 4–12% Bis-Tris gradient gels (Invitrogen/Life Technologies, Carlsbad, CA), and 3-(*N*-morpholino)-propanesulfonic acid–sodiumdodecyl sulfate buffer (Life Technologies). Proteins were transferred to a PVDF membrane (Bio-Rad). Membranes were exposed to primary anti-PS2 C-terminal (EP1515Y, Abcam, Cambridge, MA at 1:4000) and mouse anti-β-actin (Sigma-Aldrich at 1:200,000) overnight at 4°C, then exposed to the appropriate HRP-conjugated secondary antibody:donkey anti-rabbit (GE Healthcare, Piscataway, NJ at 1:1000) or sheep-anti-mouse (GE Healthcare at 1:2000) for 1 h at room temperature. Proteins were visualized with enhanced chemiluminescence (Pierce/ThermoFisher, Rockford, IL). Quantification of protein was performed employing ImageJ software (National Institutes of Health, Bethesda, MD).

Brain protein lysates were prepared by sonicating frozen brain tissue in SDS sample buffer (2% SDS, 10% glycerol, 50 mmol/L Tris-Cl, pH 6.8) on ice. Western blot analysis was performed under denaturing conditions using 4–15% gradient or 10% polyacrylamide gels (Bio-

Rad, Hercules, CA). Proteins were electroblotted onto a PVDF membrane (Bio-Rad), fixed with 0.4% paraformaldehyde for 30 min, and blocked in 5% nonfat dry milk, 0.1% Tween 20, and 0.05% thimerosal before overnight incubation at 4°C with primary antibody. Membranes were incubated with appropriate HRP-conjugated secondary antibody (1:5000; GE Healthcare, Pittsburgh, PA). Membranes were developed with Clarity Western ECL substrate (Bio-Rad) and exposed to Hyperfilm ECL (GE Healthcare).

Amyloid beta peptide analysis

Human fibroblasts were plated a density of 2×10^4 cells per well of a 96-well tissue culture-treated plate in triplicate. Conditioned media was collected at 24-, 48-, and 72-h time points and analyzed for levels of $A\beta_{1-38}$, $A\beta_{1-40}$, and $A\beta_{1-42}$ using the human (6E10) Abeta Triplex Kit (Meso Scale Discovery, Rockville, MD). Cells were subsequently lysed in the well with cell lysis buffer (Cell Signaling Technology) containing protease inhibitors. Total protein concentration for each well was determined using the Pierce BCA Protein Assay Kit (Thermo Scientific, Rockford, IL) according to the manufacturer's protocol.

Results

Case histories

Family A: proband

The patient was first evaluated in an emergency department at age 51 after concerned neighbors noted her inability to care for herself while living alone. At time of presentation, there was history of an "unspecified psychiatric disorder" with reports of a several year history of persecutory delusions. Neurological examination demonstrated poor recall, evidence of apraxia, difficulty following commands, perseveration, and disinhibition. There were no focal neurological findings. MRI showed moderate to severe cortical atrophy and severe white matter disease. At age 53, examination by a University of Washington Alzheimer Disease Research Center (UW ADRC) neurologist (J. L.) showed that she was unable to stand without assistance, had snout and palmomental reflexes, was nearly mute; she was given a diagnosis of dementia of unclear etiology. Family history was significant only for a mother reportedly diagnosed with AD (though details were not known).

Family B: proband

The patient was referred to the UW Neurogenetics clinic with a diagnosis of early-onset AD and had been previously reported by our group.[9] She had onset of cognitive impairment by age 50 and was diagnosed with AD at age 58. She had undergone a fluorodeoxyglucose-positron emission tomography (FDG-PET) brain scan, and neuropsychological examination supported a diagnosis of dementia due to AD. Given her early age of onset, genetic testing was pursued and she was found to carry PSEN2 K115Efs*11.[9] In addition to early-onset AD, she was later diagnosed with breast cancer after the original report and underwent chemotherapy. Her subsequent course was consistent with progressive memory-predominant cognitive decline; she passed at age 68.

Family B: case 2

The patient was a 42-year-old right-handed Caucasian woman and daughter of the proband. She presented to the UW ADRC endorsing subjective mild memory concerns beginning 2 years prior. She had observed difficulty recalling the exact date of her child's birthday. She frequently forgot details of significant events and needed to refer to recipes she previously knew well. She had no significant medical history. Her neurological examination was unremarkable.

Cognitive testing

The patient completed standardized cognitive testing (National Alzheimer Coordinating Center's Uniform Data Set 3 and site-specific supplemental measures) at both her initial and annual follow-up visits. Results indicated mild but significant deficits in contextual verbal memory coupled with subtler object naming difficulty and mild variability in aspects of processing speed (Table 1). Repeat evaluation demonstrated continued memory impairment but did not yield clear evidence of progressive deterioration over time. Her neurocognitive profile was deemed to be consistent with amnestic mild cognitive impairment coupled with possible early language changes, concerning for underlying Alzheimer's etiology.

Molecular imaging

The [^{18}F] florbetapir PET brain scan was negative; the lack of cortical tracer uptake was not consistent with the presence of moderate to frequent amyloid neuritic plaques.

Pathology

Family A: proband

The postmortem interval was 4 h. The fresh brain weighed 1250 g. There was mild frontoparietal and moderate

Table 1. Summary of neuropsychological measures at baseline for Family B: case 2.

Age at testing	42
WTAR estimate of premorbid intelligence	31 (39th %ile)
MoCA (max = 30)	***25 (12th %ile)***
CDR total	0.5
CDR sum of boxes	0.5
Learning and memory	
Benson Complex Figure Delayed Recall (max = 17); recognition	13; yes (46th %ile)
Craft Story 21	
Immediate recall –verbatim (max = 44)	16 ***(7th %ile)***
Immediate recall –paraphrased (max = 25)	13 ***(10th %ile)***
Delayed recall –verbatim (max = 44)	8 ***(1st %ile)***
Delayed recall –paraphrased (max = 25)	8 ***(1st %ile)***
Rey Auditory Verbal Learning Test	
Trial 1 total correct (max = 15)	5 ***(17th %ile)***
Trial 5 total correct (max = 15)	14 (81st %ile)
Trials 1–5 total correct (max = 75)	51 (49th %ile)
Trial B total correct (max = 15)	7 (68th %ile)
Trial 6 total correct (max = 15)	11 (59th %ile)
20′ free recall (max = 15)	9 (33rd %ile)
20′ recognition hits (max = 15)	13 ***(23rd %ile)***
20′ recognition false positives	2
Attention, processing speed, and executive functioning	
Trail Making Part A	20″ (45th %ile)
Trail Making Part B	48″ (46th %ile)
Span of digits forward (max = 9)	7 (56th %ile)
Span of digits backward (max = 8)	7 (89th %ile)
Letter Number Sequencing (max = 21)	12 (75th %ile)
WAIS-R Digit Symbol (max = 93)	68 (85th %ile)
Stroop (Golden) Word; errors	92, 0 ***(19th %ile)***
Stroop (Golden) Color; errors	81, 0 (61st %ile)
Stroop (Golden) Color-Word Interference; errors	42, 1 (50th %ile)
Language functioning	
Repetition (max = 2)	1
Multilingual naming test (max = 32)	28 ***(17th %ile)***
FL verbal fluency (# words)	28 (38th %ile)
Animals/minute	28 (74th %ile)
Vegetables/minute	18 (52nd %ile)
Visuospatial functioning	
Cube copy (max = 1)	0
Benson Complex Figure Copy (max = 17)	15 (26th %ile)
Benton Judgment of Line Orientation (15 item)	14 (80th %ile)

All scores represented as raw scores (percentile), with bold/italic text indicating that performance in the low average or impaired range compared to people of the same age, sex, and level of education. Limitation of the adjusted normative data for UDS measures is the small sample of same-aged subjects enrolled in NACC.

CDR, Clinical Demenita Rating; MoCA, Montreal Cognitive Assessment; NACC, National Alzheimer's Coordinating Center; UDS, Uniform Data Set; WTAR, Wechsler Test of Adult Reading.

temporal atrophy, as well as mild ventricular dilatation. There was no atrophy of the amygdala or hippocampus. Amyloid beta plaques were present in the isocortex (frontal lobe, cingulate gyrus, gyrus rectus, superior, middle, and inferior temporal lobe, inferior parietal lobe, and calcarine cortex), caudate nucleus, putamen, amygdala, hypothalamic nuclei, parahippocampal gyrus, thalamus, hippocampus, entorhinal and transentorhinal cortices, basal ganglia, and cerebellum, indicating a Thal phase 5 of 5. Neuritic plaques were frequent in the neocortex by CERAD criteria.[12] Neurofibrillary tangles were present in the CA1 in the hippocampus, subiculum, entorhinal and transentorhinal cortices, insular cortex and medial temporal cortices, basal ganglia, amygdala, locus ceruleus, and isocortex, indicating a Braak stage VI of VI. High PHF-tau burden was present in the insular cortex, medial temporal cortex, and amygdala. These findings lead to a diagnosis of AD neuropathologic change: HIGH (A3, B3, C3; see Fig. 1). There was severe cerebral amyloid angiopathy without histopathological evidence of microvascular disease. Lewy bodies and pTDP43 pathologies were not identified.

Family B: proband

The postmortem interval was 10.2 h. The fresh brain weighed 954 g. The external examination of the brain showed moderate cortical atrophy involving the frontal and temporal lobes and mild cortical atrophy involving the parietal lobes. Amyloid beta deposition was present in the isocortex, caudate nucleus, putamen, hippocampus, parahippocampal gyrus, midbrain, and cerebellum, indicating a Thal phase 5 of 5. Neuritic plaques were frequent in the neocortex by CERAD criteria. Neurofibrillary tangles were present in the CA1 in hippocampus, subiculum, entorhinal and transentorhinal cortices, insular cortex and medial temporal cortices, basal ganglia amygdala, locus ceruleus, and isocortex, indicating a Braak stage VI of VI. These findings lead to a diagnosis of AD neuropathologic change: HIGH (A3, B3, C3; see Fig. 1). Lewy bodies and pTDP43 pathologies were not identified.

Both patients show diffuse Neurofibrillary tangles deposition and dense tau neurites in the dentate gyrus, hilus, and cornu ammonis. The involvement was considered to be similar between the hippocampus and cortex. In summary, both patients showed severe and impressive pathologic changes of AD without histopathological evidence of microvascular disease.

Identification of the *PSEN2* two base-pair deletion

Genetic sequencing

We sequenced the exome of Family A Proband and 134 additional unrelated individuals with early-onset and/or

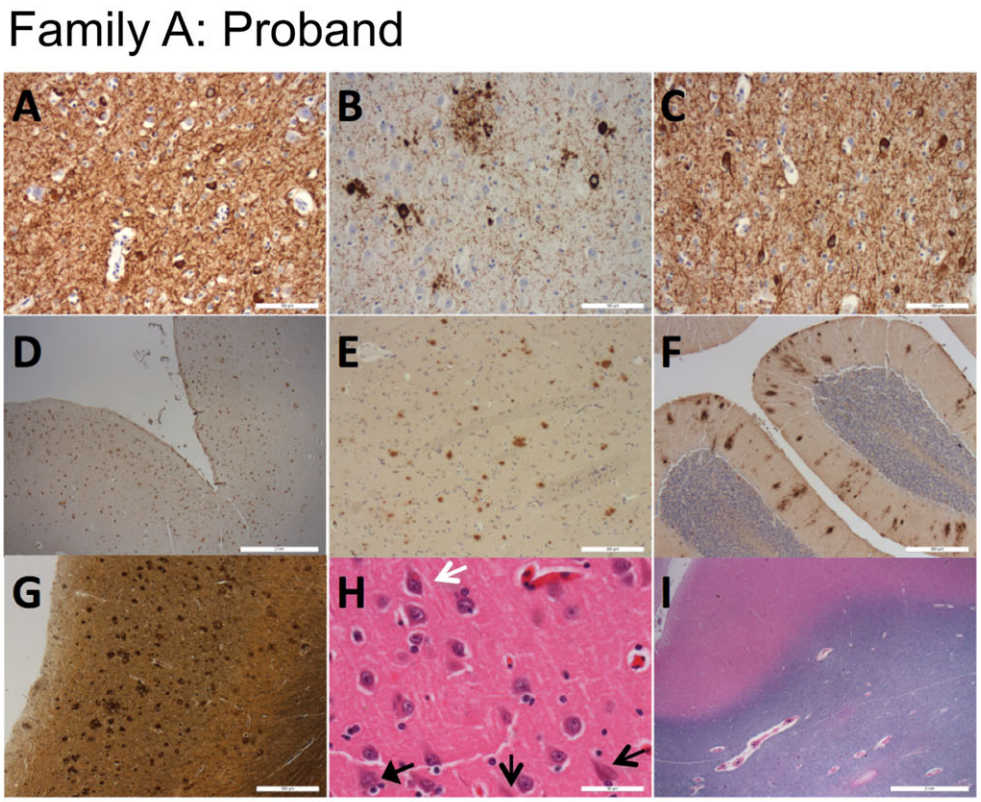

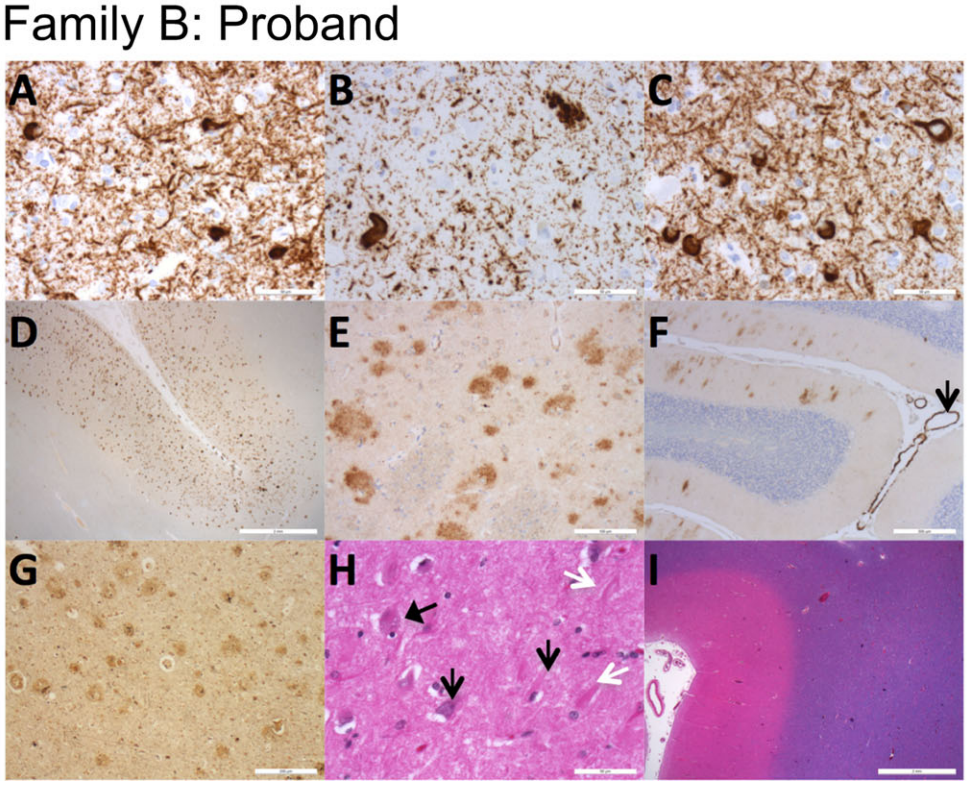

Figure 1. Family A: Proband; Neuropathologic staging. (A–C) IHC stain for PHF-tau showing increased Tau burden characterized by neurofibrillary tangles and Tau neurites. (A) Frontal lobe (40×). (B) Hilus (40×). (C) Visual cortex (40×). (D–F) IHC for β-amyloid demonstrates widespread amyloid plaques. (D) Frontal lobe (1.25×). (E) Putamen (20×). (F) Cerebellum (4×). (G) Bielschowsky stain of frontal lobe (10×) showing frequent neuritic plaques. (H) H&E/LFB stain of CA1 region (60×). Black open arrows – neurofibrillary tangles, black closed arrow – granulovacuolar degeneration, and white open arrow – Hirano body. (I) H&E/LFB of frontal lobe (1.25×) showing diffuse white matter involvement. Family B: Proband; Neuropathologic staging. (A–C) IHC stain for PHF-tau showing increased Tau burden characterized by neurofibrillary tangles and Tau neurites. (A) Frontal lobe (40×). (B) Hilus (40×). (C) Visual cortex (40×). (D–F) IHC for β-amyloid demonstrates widespread amyloid plaques. (D) Frontal lobe (1.25×). (E) Putamen (20×). (F) Cerebellum (4×). Black open arrow – amyloid angiopathy. (G) Bielschowsky stain of frontal lobe (10×) showing frequent neuritic plaques. (H) H&E/LFB stain of CA1 region (40×). Black open arrows – neurofibrillary tangles, black closed arrow – granulovacuolar degeneration, and white open arrow – "ghost tangle." (I) H&E/LFB of frontal lobe (1.25×) showing that the white matter is much less affected as compared to the first case. IHC, Immunohistochemical; PHF-tau, paired helical filament tau; H&E/LFB, hematoxylin and eosin with Luxol fast blue.

familial dementia with archived DNA. Initially, we analyzed the sequences of 38 key risk genes. The PSEN2 K115fs previously described in patient Family B Proband[9] was found in Family A Proband but not in the other 134 samples. The two base-pair deletion PSEN2 (NM_000447.2): c.342_343delGA (p.Lys115GlufsX11), genomic coordinates (b37): chr1:227071603 was confirmed using Sanger sequencing. No clinically relevant variants were found in the other 37 genes known to cause dementia or a dementia-like phenotype. We analyzed the remainder of the exome sequence data and did not identify any likely pathogenic known causative variants.

Individual Family B Case 2 carries PSEN2 K115fs initially identified in her mother (Family B Proband).[9] We detected PSEN2 K115fs by Sanger sequencing using specific primers (see Table 2). We examined the exome sequence of Family B Proband and found no pathogenic variants.

Although there is no known pedigree connection, it is possible Families A and B are related by a common ancestor. We compared the exome sequences of Family A Proband and Family B Proband. Each patient carried more than 100 rare variants, but only shared one: the PSEN2 K115fs. Although this does not rule out distant kinship, our analyses suggest that these families are not related and the PSEN2 K115fs variants may have arisen as separate events.

PSEN2 K115fs transcript is present

Early termination codon variants can be subject to nonsense-mediated decay (NMD).[18] To determine the relative PSEN2 K115fs transcript levels, we used digital droplet PCR. We observed wild-type *PSEN2* transcript in two independent wild-type controls but no variant-specific transcript (Fig. 2C). In PSEN2 K115fs patient fibroblasts, the mutant transcript is expressed at decreased levels compared to wild-type transcript suggesting that transcript instability, reduced transcription, or targeting by NMD contributes to reduced levels of the variant allele.

PS2 protein expression in patient fibroblasts

To determine the impact of PSEN2 K115fs on the expression of wild-type PS2, we analyzed patient fibroblast lysates by western blot, probing for the N-terminal and C-terminal PS2 post-endoproteolytic fragments. We detected only the wild-type copy of PS2 amino terminus fragment (Fig. 2D), which was significantly decreased in the PSEN2 K115fs fibroblasts compared to control (Fig 2E). While we predicted that the mutant transcript would result in a smaller truncated protein which could be identifiable by the N-terminal antibody, it was not detectable when using commercial N-terminus PS2 antibodies targeting the wild-type protein (Fig. 2B and D; Fig. S1). The PS2 C-terminal fragment expression is also significantly reduced in PSEN2 K115fs cells compared to wild-type controls, suggesting that in PSEN2 K115fs cells, levels of wild-type PS2 protein are decreased, consistent with decreased wild-type transcript or altered stability of PS2 C-terminus fragments in the presence of the variant allele (Fig. 2E).

Table 2. Primers.

Sanger sequencing	
Forward (with M13 tail)	TGTAAAACGACGGCCAGTCATCCAGCTCCAAATCTTCTCTACT
Reverse (with M13 tail)	CAGGAAACAGCTATGACCCTGGTGTGGAGCTGCAGGTAC
Digital droplet PCR	
PSEN2 WT, sense (5′→3′)	TGTGCGCTTCTACACAGAGAAGAAT
PSEN2 WT, anti-sense (5′→3′)	CGAGGGTGTGTCCTCAGTGAA
PSEN2 K115Efs*11, sense (5′→3′)	TGTGCGCTTCTACACAGAAGAAT
PSEN2 K115Efs*11, anti-sense (5′→3′)	CGAGGGTGTGTCCTCAGTGAA

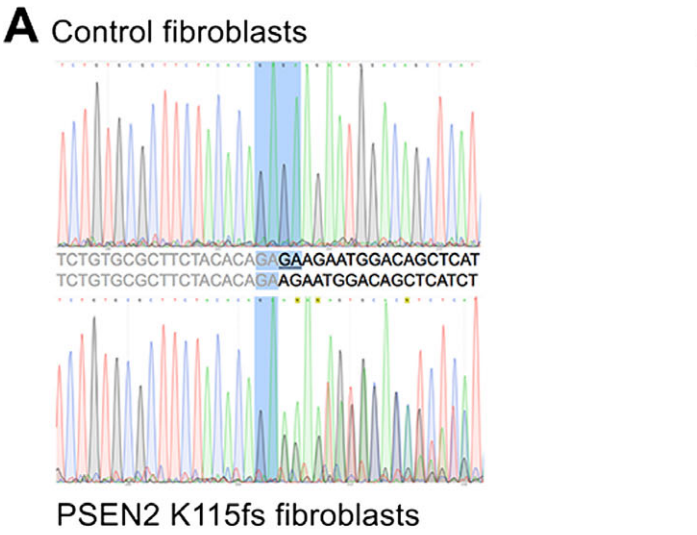

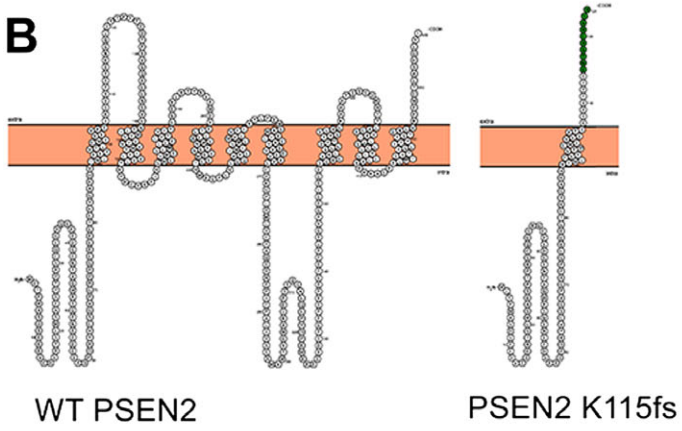

C Copies / ul cDNA (95% CI)

	WT PSEN2	Variant
WT (I)	6881.7 (6365.8 - 6900.5)	0.0 (N/A)
WT (II)	6207.3 (6143.6 - 6272.3)	0.0 (N/A)
PSEN2 K115fs	4383.9 (4282.2 - 4487.9)	2008.7 (1964.4 - 2054.0)

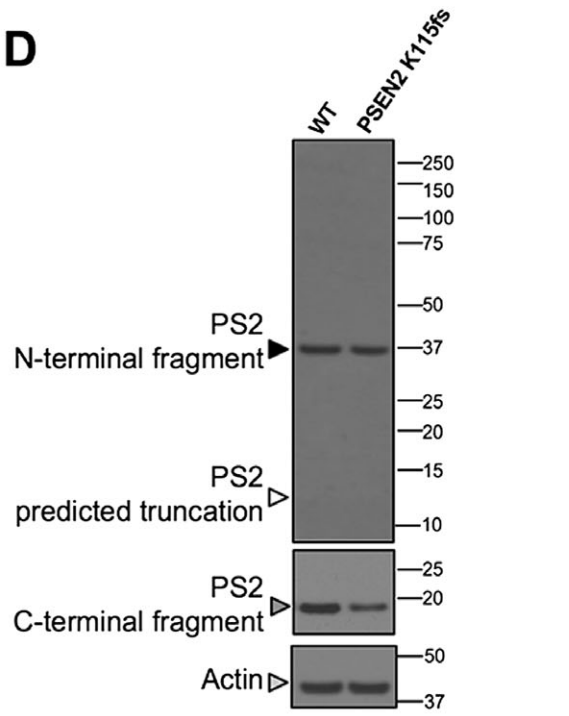

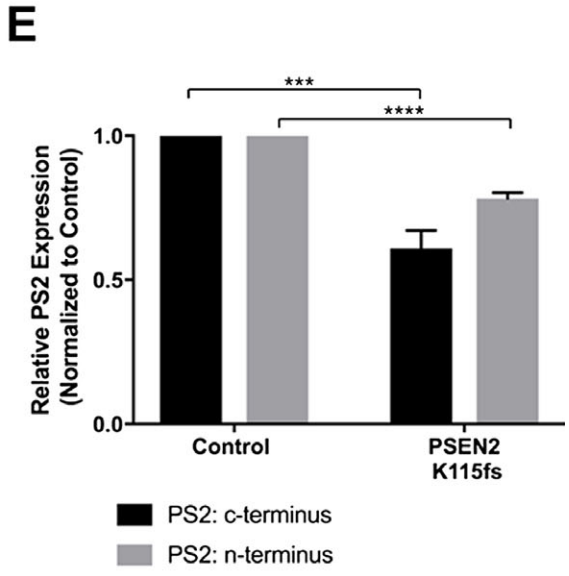

Figure 2. Fibroblast PSEN2 sequencing, transcript analysis, and protein expression. (A) Chromatogram from Sanger sequencing of Family B: Case 2. Top panel, control fibroblasts; bottom panel, PSEN2 K115Efs*11 fibroblasts. Light blue highlights the bases prior to and including the two base-pair GA deletion (underlined in control fibroblast sequence). (B) Illustration generated by Protter program simulation (http://wlab.ethz.ch/protter/start/) to demonstrate the consequences of frameshift and premature termination codon in PSEN2 K115Efs*11 compared to wild-type PS2. Dark green indicates frameshift. (C) Values and confidence intervals derived from dPCR analysis of fibroblast cDNA to compare transcript copy number between two independent wild-type cell lines and PSEN2 K115Efs*11. (D) Western blot comparing wild-type PS2N- and C-terminal fragment expression with PSEN2 K115Efs*11; note the absence of signal in the expected range for a truncated protein due to PSEN2 K115Efs*11. (E) Quantification of both N- and C-terminal PS2 fragments. Unpaired t-test: $P = 0.0008$ (C-terminus); N-terminus $P < 0.0001$. Number of replicated experiments: $n = 4$. PSEN2, presenilin 1; dPCR, digital polymerase chain reaction. ***$P < 0.001$ and ****$P < 0.0001$.

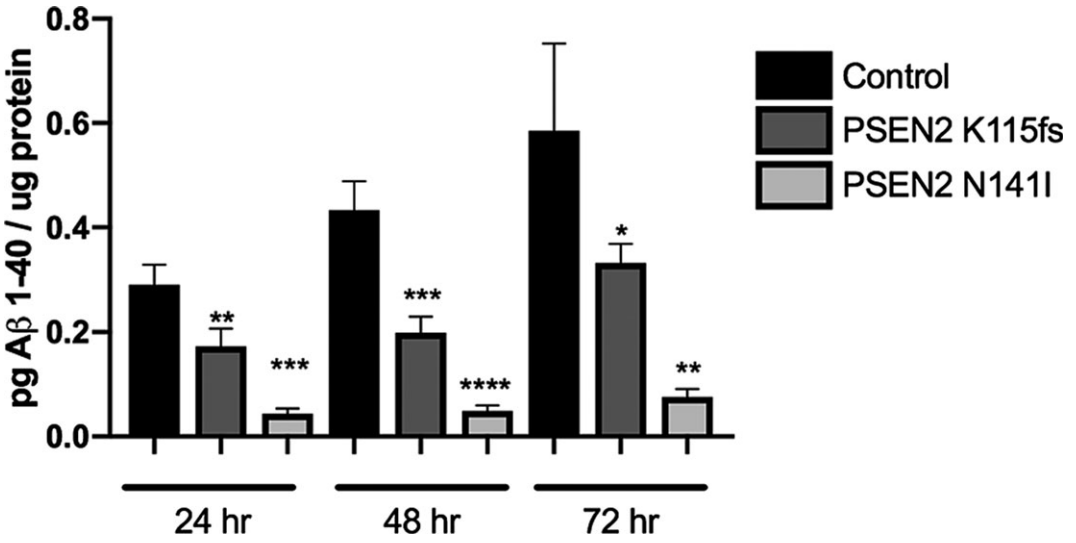

Figure 3. Analysis of the products of APP cleavage by PS2. Secreted $A\beta_{1-40}$ from conditioned media collected from wild-type, PSEN2 K115Efs*11, or PSEN2 N141I fibroblasts was analyzed at three independent time points using Meso Scale Discovery Assay, (Rockville, MD) analysis and normalized to protein concentration from each sample. Sidak statistical analyses: in comparison to WT at 24 h, $P = 0.0059$ (**) and $P = 0.0001$ (***) for PSEN2 K115fs and PSEN1 N141I, respectively. At 48 h, $P = 0.0005$ (***) and $P < 0.0001$ (****) for PSEN2 K115fs and PSEN1 N141I, respectively. At 72 h, $P = 0.0405$ (*) and $P = 0.0015$ (**) for PSEN2 K115fs and PSEN1 N141I, respectively. APP, amyloid precursor protein; PSEN2, presenilin 1.

PSEN2 K115fs enzymatic activity

Due to the decrease in expression of PS2 components necessary for enzymatic activity, we expected that γ-secretase enzymatic function would be decreased as well. To probe this function we measured the γ-secretase enzyme cleavage products of the well-known substrate, APP. In order to determine whether PSEN2 K115fs fibroblasts exhibit a decreased ability to process APP, we measured the level of secreted Aβ from control fibroblasts and PSEN2 K115fs fibroblasts at three time points (Fig. 3). In comparison to wild-type fibroblasts, PSEN2 K115fs fibroblasts secreted a decreased amount of $A\beta_{1-40}$. Secreted $A\beta_{1-40}$ is known to be decreased in cells expressing FAD-associated PSEN2 N141I, replicated here as an additional control.[19] Levels of the other Aβ peptide species $A\beta_{1-38}$ and $A\beta_{1-42}$ were below the limits of detection for this assay. To determine if the decrease in $A\beta_{1-40}$ was more likely related to impaired cleavage by PSEN2 K115fs rather than decreased substrate we measured APP transcript by real-time-PCR (RT-PCR) and by western blot, revealing similar levels of APP between the PSEN2 variant and control (Fig. S2). In addition, we assessed the impact of the PSEN2 K115fs variant on endopeptidase cleavage of *Notch1*, which is known to be impaired in cells expressing the canonical PSEN2 N141I variant.[19,20] Transcript levels of *Hes1* are an indicator of Notch intracellular domain release following γ-secretase cleavage of Notch1.[21] We found that PSEN2 K115fs fibroblasts have decreased *Hes1* levels compared to control suggestive of impaired Notch cleavage (Fig. S3). These data indicate that the PSEN2 K115fs variant alters the functional activity of PS2 similar to a known pathogenic variant in the presence of two wild-type PSEN1 alleles.

Brain-enriched PS2 isoforms

Previous studies suggest that haploinsufficiency of *PSEN1* is not sufficient to drive the molecular phenotypes of AD.[22] Furthermore, the overwhelming majority of missense variants and the notable paucity of haploinsufficiency variants linked to AD in either presenilin gene suggests that PSEN2 K115fs-associated AD is possibly driven by expression of an aberrant transcriptional product of *PSEN2*.[3] While it is possible that a small amount of the truncated protein may be responsible for driving the disease, it is also possible that the frameshift may lead to altered splicing of *PSEN2*.

A known *PSEN2* splice isoform, PS2V, excludes *PSEN2* exon 6 (previously referred to as exon 5 in original reports) and leads to a frameshift of 10 amino acids followed by a premature stop codon.[23] The generation of PS2V can be mediated in vitro by HMGA1 binding and under hypoxic incubation conditions.[23,24] Increased PS2V transcript and protein product have been detected in the

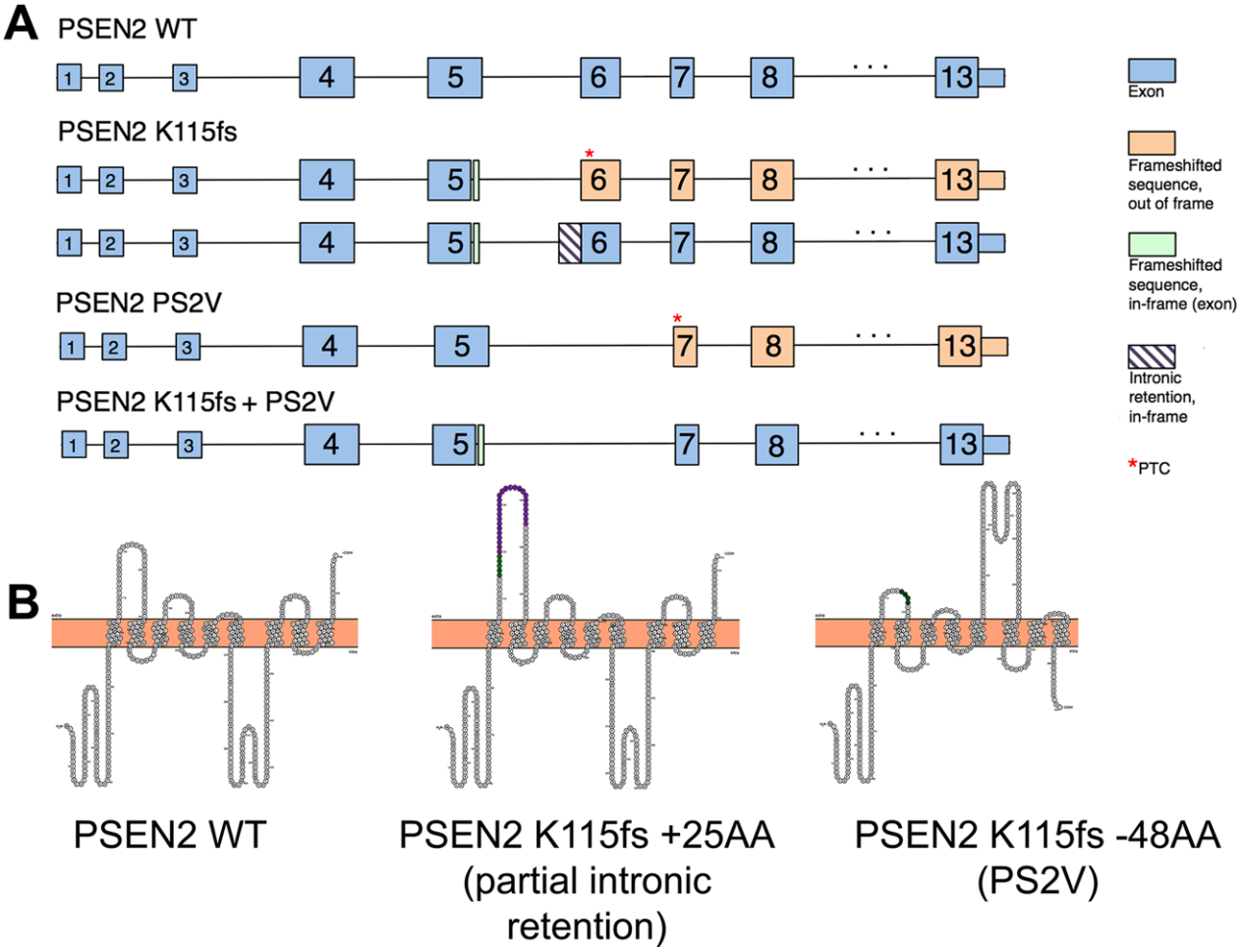

Figure 4. Consequences of alternative splicing. (A) Schematic demonstrating the predicted outcome of alternative splicing with or without the presence of PSEN2 K115Efs*11. (B) PSEN2 K115Efs*11-specific predicted addition of 25 amino acids (consequence of 77 base-pair partial intronic retention) or deletion of 48 amino acids (consequence of exon 6 exclusion) after the first PS2 transmembrane domain (generated with the Protter program simulation, http://wlab.ethz.ch/protter/start/).[46] Dark green indicates frameshift, while purple indicates the region of 25 inserted amino acids.

brains of patients with sporadic AD suggesting a possible role in AD pathogenic processes.[23,25] The mechanism by which PS2V influences AD pathogenesis remains unclear though its presence in AD brain raises the possibility that altered splice forms of FAD genes may contribute to AD pathogenesis. Several PS FAD-associated variants also generate alternatively spliced isoforms, producing unexpected products.[26–29] Therefore, we sought to determine if PSEN2 K115fs transcript results in alternatively spliced isoforms that could produce a novel deleterious protein.

We designed primers to capture alternative splicing that might occur between exons 5 and 7 (Fig. 4A; Fig. S4), which would also capture loss of exon 6 (PS2V). We amplified cDNA from wild-type PSEN2, PSEN2 K115fs, and PSEN2 N141I fibroblast RNA using primers flanking exon 6. While a product of the expected size was present, no alternative banding pattern was evident, suggesting that alternative splicing is not robust at this region in fibroblasts (Fig. 5).

To determine whether alternative splicing might occur at this site in a more disease-relevant tissue, we isolated RNA and generated cDNA from PSEN2 K115fs brain lysate. In addition to the expected band, we found two additional bands of both larger and smaller size than the original band. Upon sequencing by TOPO cloning, we determined that the larger band represents a 77 base-pair partial intronic retention (Figs. 4A, 5). The smaller size band resulted from the loss of exon 6, representing the PS2V isoform (Figs. 4A, 5). Intriguingly, these alternative isoforms are not PSEN2 K115fs patient specific. Using RT-PCR specific for detection of the partial intronic retention isoform, we determined that a small percentage of *PSEN2* transcripts spliced in this manner are present in both Sporadic AD

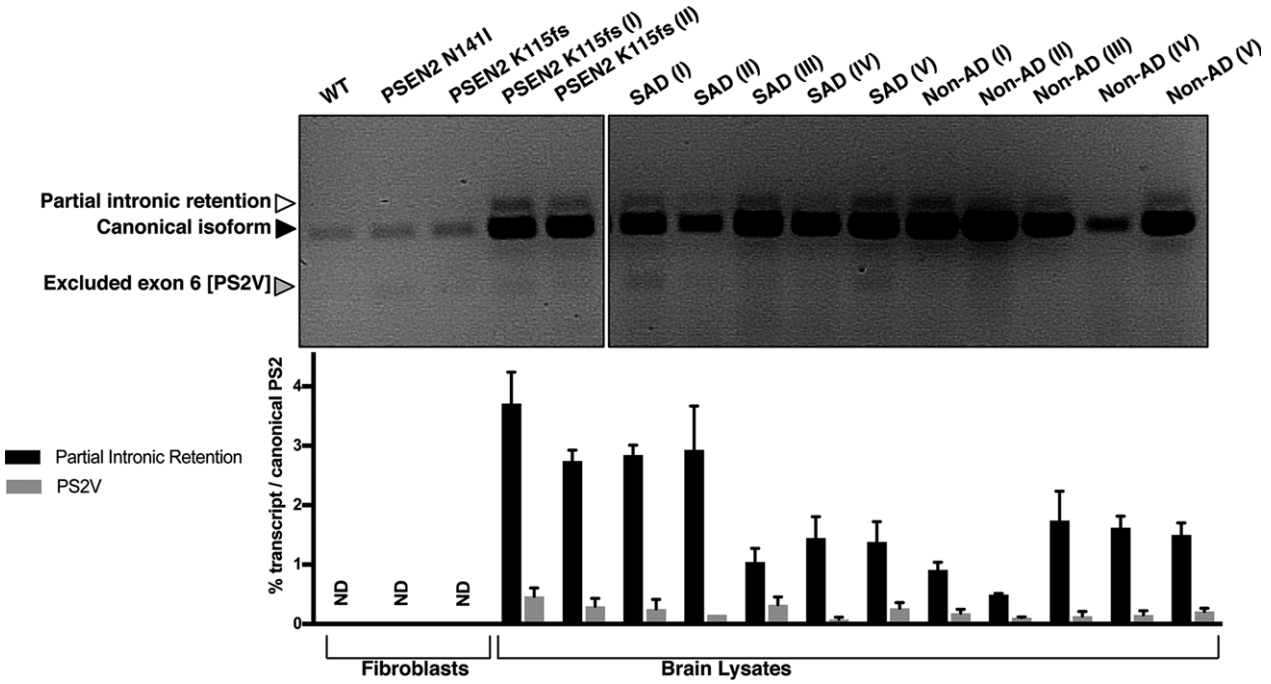

Figure 5. Alternative transcripts are present in brain-specific lysates. Top: PCR amplification of cDNA from brain lysates between exons 5 and 7 show two alternatively spliced products above and below a main PSEN2 band. Bottom: RT-PCR quantification of alternatively spliced products. RT-PCR, real-time polymerase chain reaction; PSEN2, presenilin 1.

(SAD) and Familial AD (FAD) brain lysate as well as in control brain (Fig. 5). Of note, one SAD case with levels of the 77 base-pair partial intronic retention transcript similar to PSEN2 K115fs (Fig. 5, SAD II) had an early age-of-onset at 50 years and was found to carry the *PSEN2* R62H variant previously suggested to be an age-of-onset modifier.[30]

Upon analyzing the sequence surrounding the exon 6 splice acceptor site in a splice site prediction program human splicing finder (http://www.umd.be/HSF3/), we found that surprisingly, the site corresponding to a 77-nucleotide insertion has a greater context score than the canonical splice acceptor site. Thus, one or more proteins involved in suppressing silencing likely prevent use of the upstream splice acceptor. In the context of aging or in the brain, the mechanism to prevent inclusion of the upstream splice acceptor may be weakened over time. By using RNA sequencing data deposited from the Mount Sinai Brain Bank, we confirmed that 20 of 165 sequenced anterior frontal cortex samples had reads that overlapped the upstream 77-nucleotide splice acceptor site, providing independent verification of the utilization of this splice site.

The deletion of two nucleotides in the PSEN2 K115fs allele leads to expression of both the partial intronic retention and PS2V transcripts, which enables return to the original reading frame following a short frameshift. The partial intronic retention is predicted to result in a 25-amino acid insertion into the loop between the first and second transmembrane domains (Fig. 4B, Fig. S5). Similarly, the exclusion of exon 6 (PS2V) isoform is predicted to return to the original reading frame after a short frameshift, which would instead cause a 48-amino acid deletion and predicted loss of the entire second transmembrane domain (Fig. 4B, Fig. S5). These altered transcripts are predicted to be translated into full-length proteins due to the presence of the two absent base pairs of the PSEN2 K115fs allele.

Brain PS2 protein expression

Due to the predicted insertion or deletion of large peptide sequences, either protein product generated from alternative PS2 isoforms may impact the structure and/or function of PSEN2 K115fs within the brain. Furthermore, the presence of these alternative products may act in a dominant-negative fashion against wild-type PS2. Therefore, we sought to determine whether we could detect the presence of these protein products in brain lysate. While we did not detect these alternative products by western blot of PSEN2 K115fs brain lysate (Fig. 6), this could be due to lack of antibody specificity, insufficient resolution due to a size difference of 2–3kD, or low level of expression due to low transcript abundance.

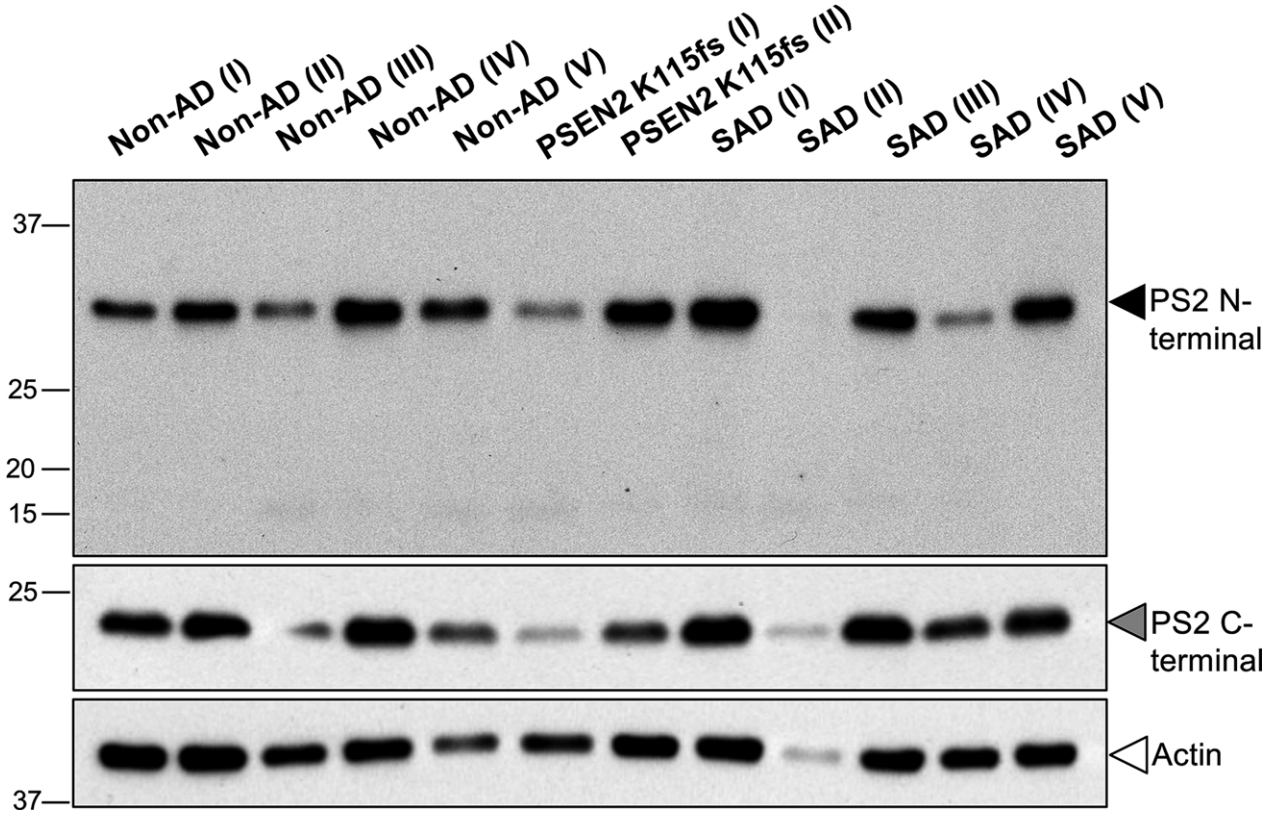

Figure 6. Western blot of brain lysates. Wild-type PS2 protein is detected by both N- and C-terminal antibodies.

Discussion

We report strong evidence supporting pathogenicity of a two base-pair *PSEN2* deletion variant in two individuals with neuropathologically documented early-onset AD. The majority of reported FAD-associated variants in the presenilin genes are missense[3] and hypothesized to process amyloid and other substrates abnormally.[4] Our analysis of fibroblast-secreted Aβ data suggests that, like PSEN2 N141I, PSEN2 K115fs imparts a biochemical loss-of-function phenotype (Fig. 3). We have confirmed the presence of the transcribed PSEN2 K115fs allele and demonstrate that this pathogenic variant undergoes alternative splicing detectable in brain using semiquantitative measures. The alternative transcripts are predicted to generate structurally and functionally altered PS2 protein products, which may contribute to the development of AD. The proposed pathogenic mechanism(s) leading to AD driven by *PSEN* variants are complex[31]; our studies suggest at least three mechanisms by which the molecular change in PSEN2 described here could lead to neural dysfunction.

1. Loss of normal PS2 function. The observed biochemical alterations noted in patient fibroblasts may be explained by the decreased dose of wild-type PS2 protein. Congruent with this model, wild-type PS2 expression is significantly reduced by western blot (Fig. 2E). We detected decreased levels of both N- and C-terminal fragments in patient lysates, and a stronger impact on C-terminus levels which may reflect differential stability or susceptibility to degradation. Previous work has demonstrated that PS fragments are rapidly degraded when not incorporated into a heterodimer and thus alterations of heterodimer or γ-secretase complex stoichiometry in PSEN2 variant cells may influence detectable levels of PS2 fragments.[32]

2. Expression of truncated PS2 protein: The loss of two base pairs in PSEN2 K115fs would lead to a frameshift followed by a premature stop codon. This transcript is predicted to generate a severely truncated PS2 protein product. In silico analyses suggest that the location of the two base-pair deletion marks the transcript as a canonical target for NMD because the premature stop codon induced by the frameshift is located more than 50 nucleotides upstream of a splice junction.[18] We did detect the PSEN2 K115fs allele (Fig. 2C) though whether the transcript is stable or escapes eventual NMD mediated degradation was not assayed in these studies. If the shortened transcript was expressed at low levels and translated, a

PSEN2 K115fs truncated protein would only retain one of eight transmembrane domains, lacking both the endoproteolytic and catalytic sites of PS2 (Fig. 2B, Fig. S5). Similarly, the known PS2 splice isoform PS2V, which excludes PS2 exon 6, also leads to a frameshift followed by a premature stop codon.[23] Because of the clear similarity between PSEN2 K115fs and PS2V, it is possible that, like PS2V, low-level truncated PSEN2 K115fs protein expression might be linked to disease. With commercial antibodies, we were unable to detect expression of a truncated PSEN2 K115fs fragment (Fig. 2D). It is possible that a truncated peptide could be expressed below the limit of detection by this assay or other mechanisms may diminish the expression of the transcript product. As was required for detection of the PS2V protein isoform, detection of the truncated PSEN2 K115fs may require creation of a peptide-specific antibody.[25]

3. Expression of brain tissue enriched PS2 splice forms: We hypothesized that alternative splicing may be responsible for the generation of one or more novel, deleterious protein products. As previously discussed, *PSEN2* is known to undergo alternative splicing, generating the PS2V isoform through exon 6 exclusion.[23] Several pathogenic *PSEN1* variants also employ alternative splicing, such as the mutation of a splice donor site to generate alternative transcripts as well as exon exclusion.[27,28] Furthermore, global transcriptomics studies have revealed that alternative splicing occurs most often in brain tissue[33,34]; therefore, it is likely that alternative splicing could impact several presenilin variants in previously unexplored ways. To examine whether PSEN2 K115fs generated alternatively spliced transcripts, we PCR-amplified cDNA using primers upstream and downstream of exon 6. While alternative splicing was not detectable at this site in fibroblasts using semiquantitative methods, we found a novel partial intronic retention transcript as well as PS2V in brain lysate. These transcripts were not unique to PSEN2 K115fs, as they were also found in FAD, sporadic, and non-AD age-matched control brain lysates. In silico, the aforementioned alternatively spliced transcripts found in sporadic AD and non-AD control would not be translated into full-length PS2 due to a frameshift leading to a premature stop codon. Interestingly, in the context of PSEN2 K115fs, both alternative transcripts would return to the original reading frame. The PSEN2 K115fs partial intronic retention transcript is predicted to express a 25-amino acid insertion after the first transmembrane domain, while PS2V exon 6 loss is predicted to cause 48-amino acid loss and an entire transmembrane domain (Fig. 4B, Fig. S5). The expression of either alternative protein was below the limit of detection by western blot. This may be due to the low percentage or instability of the proteins, additional undetected alternative splicing downstream in the transcripts, or inability of the antibody to recognize the altered protein products. These alternative PS2 protein structures could impact substrate processing, protein folding, subcellular localization, and γ-secretase complex formation in unanticipated ways. For example, FAD-associated presenilin mutant proteins have been demonstrated to act in a dominant-negative way by heterooligomerizing with wild-type presenilin.[35]

Alternative splicing of AD risk genes in sporadic AD

Alternative splicing of *PSEN2* in the context of an AD-associated variant could lead to the expression of deleterious protein products. However, these alternative splicing events are not unique to PSEN2 K115fs. Changes in neuronal synaptic function during aging are linked to alternative splicing and may also contribute to disease.[36] Alternative splicing confers transcriptomic and protein complexity to brain tissue, increasing both with age and in AD.[33,37,38] Several groups have found that genes such as *APP*, *Tau*, *APOE*, and *ABCA7* can undergo alternative splicing, potentially increasing risk for disease.[38,39] Other splice machinery alterations can impact APP processing of Aβ indirectly through alternative splice-driven changes in function, such as transcription factors and regulators like *RbFox1*.[38] Frameshifted proteins resulting from acquired dinucleotide deletions (ΔGA or ΔGU) in APP and Ubiquitin mRNA have also been associated with SAD pathology and suggested to contribute to AD pathogenesis.[40,41] Thus, our data complement the growing body of work suggesting that alternative splicing or RNA editing in brain tissue may be a relevant component of AD pathogenesis.

Protein products resulting from presenilin alternative splicing could be responsible for contributing to AD. Similar variants previously categorized as unknown significance due to unclear mechanisms may also induce or undergo alternative splicing, and further study is merited in these cases. Of note, a recent publication highlighted the discovery of an additional *PSEN2* frameshift variant concluded to be of unknown significance found in two individuals with AD. The identified one base-pair deletion variant in *PSEN2* was also found to generate altered splice forms and resulted in decreased wild-type PS2 protein in brain tissue.[42] Characterizing the full variation in mechanism through the study of noncanonical variants will aid in understanding the mechanism of FAD as well as of sporadic AD. Alternatively spliced products may impact the molecular phenotypes of AD in vitro, such as the secretion of Aβ, phosphorylation of tau, electrophysiological properties, or the susceptibility to hypoxia and/or other environmental or aging-related insults.

Although the amyloid PET scan of Family B Case 2 did not demonstrate the presence of moderate to severe

cortical amyloid neuritic plaques, it is possible that this individual does not yet have a burden of fibrillar amyloid pathology that reaches the threshold of detection. Individuals with symptomatic FAD lacking evidence of fibrillar amyloid deposition on amyloid imaging have been reported previously.[43,44] Additionally, binding affinity of amyloid radiotracers has been found to be variable for different FAD-associated variants.[45]

Conclusion

Our study highlights the importance of considering the impact of alternative splicing of *PSEN* and other AD-related genes. Further studies to explore mechanistic impact of mRNA and protein isoforms associated with PSEN2 K115Efs*11 will benefit from extension to physiologically disease-relevant cell types. Our study highlights, through the analyses of multiple tissue types, the complexity of investigating *PSEN* variant mechanisms in AD.

Acknowledgments

We thank the members of the University of Washington Medicine Center for Precision Diagnostics for technical support, the Geriatric Research, Education, and Clinical Center at the VA Puget Sound Health Care System and University of Washington's Alzheimer Disease Research Center. We also thank Kathryn Gudsnuk and Sarah Peterson for technical support.

Author Contributions

J. E. B., S. A. B., M. M. C., R. S. M., G. A. G., M. L., J. E. Y., P. N. V., T. B., and S. J. conceived and designed the study; J. E. B., S. A. B., C. L. S., B. S., L. O., M. M. C., K. S., C. K., K. D. R., T. G., C. C., K. R., D. T., J. L., K. S., C. L., C. D. K., L. F. G. C., R. S. M., S. H. M. N., M. N., M. L., M. D., J. E. Y., and P. N. V. acquired and analyzed the data; and J. E. B., S. A. B., B. S., M. M. C., C. K., K. D. R., C. C., K. R., C. L., L. F. G. C., R. S. M., S. H. M. N., M. N., M. L., J. E. Y., P. N. V., T. B., and S. J. contributed to writing the manuscript.

Conflicts of Interest

The authors have no conflicts of interest to disclose.

References

1. Bird TD. Early-onset familial Alzheimer disease [Internet]. 1993. Available from: http://www.ncbi.nlm.nih.gov/pubmed/20301414 (accessed April 26, 2018).
2. Lippa CF, Saunders AM, Smith TW, et al. Familial and sporadic Alzheimer's disease: neuropathology cannot exclude a final common pathway. Neurology 1996;46:406–412.
3. Cruts M, Theuns J, Van Broeckhoven C. Locus-specific mutation databases for neurodegenerative brain diseases. Hum Mutat 2012;33:1340–1344.
4. De Strooper B, Iwatsubo T, Wolfe MS. Presenilins and γ-secretase: structure, function, and role in Alzheimer disease. Cold Spring Harb Perspect Med 2012;2: a006304.
5. Weggen S, Beher D. Molecular consequences of amyloid precursor protein and presenilin mutations causing autosomal-dominant Alzheimer's disease. Alzheimers Res Ther 2012;4:9.
6. Chávez-Gutiérrez L, Bammens L, Benilova I, et al. The mechanism of γ-secretase dysfunction in familial Alzheimer disease. EMBO J 2012;31:2261–2274.
7. Szaruga M, Munteanu B, Lismont S, et al. Alzheimer's-causing mutations shift Aβ length by destabilizing γ-secretase-Aβn interactions. Cell 2017;170:443–456.e14.
8. De Strooper B. Loss-of-function presenilin mutations in Alzheimer disease. Talking Point on the role of presenilin mutations in Alzheimer disease. EMBO Rep 2007;8:141–146.
9. Jayadev S, Leverenz JB, Steinbart E, et al. Alzheimer's disease phenotypes and genotypes associated with mutations in presenilin 2. Brain 2010;133:1143–1154.
10. Hyman BT, Phelps CH, Beach TG, et al. National Institute on Aging-Alzheimer's Association guidelines for the neuropathologic assessment of Alzheimer's disease. Alzheimers Dement 2012;8:1–13.
11. Montine TJ, Phelps CH, Beach TG, et al. National Institute on Aging-Alzheimer's Association guidelines for the neuropathologic assessment of Alzheimer's disease: a practical approach. Acta Neuropathol 2012;123:1–11.
12. Mirra SS, Heyman A, McKeel D, et al. The Consortium to Establish a Registry for Alzheimer's Disease (CERAD). Part II. Standardization of the neuropathologic assessment of Alzheimer's disease. Neurology 1991;41:479–486.
13. McKenna A, Hanna M, Banks E, et al. The Genome Analysis Toolkit: a MapReduce framework for analyzing next-generation DNA sequencing data. Genome Res 2010;20:1297–1303.
14. DePristo MA, Banks E, Poplin R, et al. A framework for variation discovery and genotyping using next-generation DNA sequencing data. Nat Genet 2011;43:491–498.
15. Vogelstein B, Kinzler KW. Digital PCR. Proc Natl Acad Sci USA 1999;96:9236–9241.
16. De St. Groth SF. The evaluation of limiting dilution assays. J Immunol Methods 1982;49:R11–R23.
17. Shao S, Zhao X, Zhang X, et al. Notch1 signaling regulates the epithelial-mesenchymal transition and invasion of breast cancer in a Slug-dependent manner. Mol Cancer 2015;14:28.

18. Popp MW, Maquat LE. Leveraging rules of nonsense-mediated mRNA decay for genome engineering and personalized medicine. Cell 2016;165:1319–1322.
19. Walker ES, Martinez M, Brunkan AL, Goate A. Presenilin 2 familial Alzheimer's disease mutations result in partial loss of function and dramatic changes in Abeta 42/40 ratios. J Neurochem 2005;92:294–301.
20. Sannerud R, Esselens C, Ejsmont P, et al. Restricted location of PSEN2/γ-secretase determines substrate specificity and generates an intracellular Aβ pool. Cell 2016;166:193–208.
21. Moriyama M, Osawa M, Mak S-S, et al. Notch signaling via Hes1 transcription factor maintains survival of melanoblasts and melanocyte stem cells. J Cell Biol 2006;173:333–339.
22. Woodruff G, Young JE, Martinez FJ, et al. The presenilin-1 ΔE9 mutation results in reduced γ-secretase activity, but not total loss of PS1 function, in isogenic human stem cells. Cell Rep 2013;5:974–985.
23. Sato N, Hori O, Yamaguchi A, et al. A novel presenilin-2 splice variant in human Alzheimer's disease brain tissue. J Neurochem 1999;72:2498–2505.
24. Manabe T, Katayama T, Sato N, et al. Induced HMGA1a expression causes aberrant splicing of presenilin-2 pre-mRNA in sporadic Alzheimer's disease. Cell Death Differ 2003;10:698–708.
25. Sato N, Imaizumi K, Manabe T, et al. Increased production of β-amyloid and vulnerability to endoplasmic reticulum stress by an aberrant spliced form of presenilin 2. J Biol Chem 2001;276:2108–2114.
26. Perez-Tur J, Froelich S, Prihar G, et al. A mutation in Alzheimer's disease destroying a splice acceptor site in the presenilin-1 gene. Neuroreport 1995;7:297–301.
27. De Jonghe C, Cruts M, Rogaeva EA, et al. Aberrant splicing in the presenilin-1 intron 4 mutation causes presenile Alzheimer's disease by increased Abeta42 secretion. Hum Mol Genet 1999;8:1529–1540.
28. Kwok JBJ, Halliday GM, Brooks WS, et al. Presenilin-1 mutation L271V results in altered exon 8 splicing and Alzheimer's disease with non-cored plaques and no neuritic dystrophy. J Biol Chem 2003;278:6748–6754.
29. Le Guennec K, Veugelen S, Quenez O, et al. Deletion of exons 9 and 10 of the presenilin 1 gene in a patient with early-onset Alzheimer disease generates longer amyloid seeds. Neurobiol Dis 2017;104:97–103.
30. Cruchaga C, Chakraverty S, Mayo K, et al. Rare variants in APP, PSEN1 and PSEN2 increase risk for AD in late-onset Alzheimer's disease families. PLoS One 2012;7: e31039.
31. Jayne T, Newman M, Verdile G, et al. Evidence for and against a pathogenic role of reduced γ-secretase activity in familial Alzheimer's disease. J Alzheimers Dis 2016;52:781–799.
32. Steiner H, Capell A, Pesold B, et al. Expression of Alzheimer's disease-associated presenilin-1 is controlled by proteolytic degradation and complex formation. J Biol Chem 1998;273:32322–32331.
33. Twine NA, Janitz K, Wilkins MR, Janitz M. Whole transcriptome sequencing reveals gene expression and splicing differences in brain regions affected by Alzheimer's disease. PLoS One 2011;6:e16266.
34. Yeo G, Holste D, Kreiman G, Burge CB. Variation in alternative splicing across human tissues. Genome Biol 2004;5:R74.
35. Zhou R, Yang G, Shi Y. Dominant negative effect of the loss-of-function γ-secretase mutants on the wild-type enzyme through heterooligomerization. Proc Natl Acad Sci USA 2017;114:12731–12736.
36. Stilling RM, Benito E, Gertig M, et al. De-regulation of gene expression and alternative splicing affects distinct cellular pathways in the aging hippocampus. Front Cell Neurosci 2014;8:373.
37. Mazin P, Xiong J, Liu X, et al. Widespread splicing changes in human brain development and aging. Mol Syst Biol 2013;9:633.
38. Love JE, Hayden EJ, Rohn TT. Alternative splicing in Alzheimer's disease. J Parkinsons Dis Alzheimers Dis 2015;2:6.
39. De Roeck A, Duchateau L, Van Dongen J, et al. An intronic VNTR affects splicing of ABCA7 and increases risk of Alzheimer's disease. Acta Neuropathol 2018;135:827–837.
40. van Leeuwen FW, de Kleijn DP, van den Hurk HH, et al. Frameshift mutants of beta amyloid precursor protein and ubiquitin-B in Alzheimer's and Down patients. Science 1998;279:242–247.
41. van Leeuwen FW, van Tijn P, Sonnemans MAF, et al. Frameshift proteins in autosomal dominant forms of Alzheimer disease and other tauopathies. Neurology 2006;66(2 suppl 1):S86–S92.
42. Perrone F, Cacace R, Van Mossevelde S, et al. Genetic screening in early-onset dementia patients with unclear phenotype: relevance for clinical diagnosis. Neurobiol Aging 2018;69:292.e7–292.e14.
43. Tomiyama T, Nagata T, Shimada H, et al. A new amyloid beta variant favoring oligomerization in Alzheimer's-type dementia. Ann Neurol 2008;63:377–387.
44. Kutoku Y, Ohsawa Y, Kuwano R, et al. A second pedigree with amyloid-less familial Alzheimer's disease harboring an identical mutation in the amyloid precursor protein gene (E693delta). Intern Med 2015;54:205–208.
45. Balamurugan K, Murugan NA, Långström B, et al. Effect of Alzheimer familial chromosomal mutations on the amyloid fibril interaction with different PET tracers: insight from molecular modeling studies. ACS Chem Neurosci 2017;8:2655–2666.
46. Omasits U, Ahrens CH, Müller S, Wollscheid B. Protter: interactive protein feature visualization and integration

with experimental proteomic data. Bioinformatics 2014;30:884–886.

Supporting Information

Additional supporting information may be found online in the Supporting Information section at the end of the article.

Figure S1. Location of epitopes for western blotting.
Figure S2. APP and Notch levels do not differ significantly between control and PSEN2 K115fs fibroblasts.
Figure S3. *Hes1* expression in fibroblasts with and without Jagged stimulation of Notch.
Figure S4. Real-time PCR schematic.
Figure S5. Amino acid changes as a result of PSEN2 K115fs.

